

# First Principles Calculation of Ballistic Current from Electron-Hole Interaction

Zhenbang Dai<sup>1</sup> and Andrew M. Rappe<sup>1</sup>

<sup>1</sup>*Department of Chemistry, University of Pennsylvania, Philadelphia, Pennsylvania 19104-6323, USA*  
(Dated: May 3, 2022)

The bulk photovoltaic effect (BPVE) has attracted an increasing interest due to its potential to overcome the efficiency limit of traditional photovoltaics, and much effort has been devoted to understanding its underlying physics. However, previous work has shown that theoretical models of the shift current and the phonon-assisted ballistic current in real materials do not fully account for the experimental BPVE photocurrent, so other mechanisms should be investigated in order to obtain a complete picture of BPVE. In this Letter, we demonstrate two approaches that enable the *ab initio* calculation of the ballistic current originating from the electron-hole interaction in semiconductors. Using BaTiO<sub>3</sub> and monolayer MoS<sub>2</sub> as two examples, we show clearly that for them the asymmetric scattering from electron-hole interaction is less appreciable than that from electron-phonon interaction, indicating more scattering processes need to be included to further improve the BPVE theory. Moreover, we provide a first-principles approach for material prediction and design in order to search for materials with larger ballistic current due to electron-hole interactions.

**Keywords:** BPVE, shift current, ballistic current, first principles, electron-hole interaction, exciton

*Introduction.*— The bulk photovoltaic effect (BPVE) describes the generation of dc photocurrent in a homogeneous material, in contrast to traditional photovoltaic effects where a heterojunction is usually needed. [1] Such phenomenon requires the breaking of inversion symmetry or time-reversal symmetry, but it is not restricted by the upper limit of efficiency imposed on traditional solar cells. The BPVE can provide a large open-circuit photovoltage, thus attracting an increasing interest in the past few years in the field of opto-electronics. [2, 3] On the other hand, the underlying physics of the BPVE is still under debate. A first-principles calculation suggested that the shift current [4], which describes the coordinate shift during the optical excitation process, is the dominant mechanism in BaTiO<sub>3</sub> [5], but more recent first-principles studies showed that shift current only contributes a portion (perhaps still a majority) of the total BPVE current. [6] Therefore, other processes have to be considered as well in order to have a complete description of BPVE.

Another important mechanism for the BPVE has been proposed and studied, the *ballistic current* (BC). [1] Ballistic current originates from the asymmetric carrier generation at  $\mathbf{k}$  and  $-\mathbf{k}$ , which in turn will induce a net current. The asymmetric carrier generation can be attributed to coherent scatterings from multiple contributions, such as the electron-phonon interaction, electron-hole interaction, and defects. It was reported that the ballistic current due to electron-hole scattering largely rationalized the photocurrent near the band edge in GaAs. [7] Recently, we have shown that the ballistic current arising from the intrinsic electron-phonon interaction can have comparable magnitude with the shift current, enhancing the overall agreement of the theoretical and experimental BPVE spectra, though some discrepancy still persists. [8] Thus, it is of great interest to explore other contributions to ballistic current and under-

stand their importance toward the overall BPVE phenomenon. Due to the complexity of BPVE, a general rule of thumb for determining the contributions from various mechanisms is difficult to obtain, so establishing a paradigm for numerical evaluation of these mechanisms will be crucial to resolve the controversies over shift current and ballistic current.

In this Letter, we use first-principles calculations to investigate the asymmetric carrier generation in semiconductors from another intrinsic scattering process, the electron-hole scattering. We include Coulomb interactions between the electrons excited to the conduction band and the holes left in the valence band across the whole Brillouin zone, which goes beyond previous treatment where only band extremum states are considered [9]. Such generalization is crucial to a correct understanding of Coulomb interaction in contributing the BPVE since without it, the neglect of other  $\mathbf{k}$  points and bands could obscure the evaluation of different BPVE mechanisms in a broader range of light frequency. The Coulomb interaction is known to give rise to exciton states, which greatly modify the optical properties of materials, and it can also lead to asymmetric scattering of carriers. [10] Due to the intimate relation to excitons, we will call the current from electron-hole interactions the *exciton ballistic current* (ex-BC). The current can be calculated within a Boltzmann transport model:

$$j^{\alpha\beta,\gamma}(\omega) = 2e\tau_0 \sum_{cv\mathbf{k}} \Gamma_{cv,\mathbf{k}}^{\alpha\beta}(\omega) [v_{c\mathbf{k}}^{e,\gamma} - v_{v\mathbf{k}}^{e,\gamma}] \quad (1)$$

where  $\Gamma_{cv,\mathbf{k}}^{\alpha\beta}$  is the carrier generation rate for an electron-hole pair ( $c, v$ ) at  $\mathbf{k}$ ,  $e$  is the electron charge,  $\tau_0$  is the momentum relaxation time, and  $\mathbf{v}_{c\mathbf{k}}^e$  ( $\mathbf{v}_{v\mathbf{k}}^e$ ) is the electron (hole) velocity obtained from band derivatives. The main task is to calculate  $\Gamma_{cv,\mathbf{k}}^{\alpha\beta}(\omega)$ , and we take two approaches to tackle this problem: a diagrammatic approach which has been widely used to describe Wannier

excitons [11, 12], and a many-body approach that largely resembles the modern *ab initio* way of computing exciton states. [10, 13] We implement these two approaches via first-principles theory and compare the results with shift current and phonon-assisted ballistic current (ph-BC). The first-principles results show clearly that for BaTiO<sub>3</sub> and monolayer 2H-MoS<sub>2</sub> (which we refer to as MoS<sub>2</sub> hereafter), the ex-BC only makes a minor contribution to the overall BPVE.

*Diagrammatic approach.*— We first derive an expression for ex-BC from a phenomenological treatment that is widely used when investigating Wannier excitons. The model starts by assuming a single-particle Hamiltonian for the unperturbed state and taking the electron-hole interaction as a perturbation:

$$H_0 = \sum_{c\mathbf{k}} \epsilon_{c\mathbf{k}} \hat{c}_{c\mathbf{k}}^\dagger \hat{c}_{c\mathbf{k}} + \sum_{v\mathbf{k}} \epsilon_{v\mathbf{k}} \hat{b}_{v\mathbf{k}}^\dagger \hat{b}_{v\mathbf{k}} \quad (2)$$

$$V_{\text{int}} = - \sum_{cc'vv'} \sum_{\mathbf{k}\mathbf{k}'\mathbf{q}} V_{\mathbf{q}}^{cc',vv'} \hat{c}_{c\mathbf{k}+\mathbf{q}}^\dagger \hat{b}_{v-\mathbf{k}'-\mathbf{q}}^\dagger \hat{b}_{v'-\mathbf{k}'} \hat{c}_{c'\mathbf{k}}, \quad (3)$$

where  $\hat{c}_{c\mathbf{k}}^\dagger$  ( $\hat{c}_{c\mathbf{k}}$ ) and  $\hat{b}_{v\mathbf{k}}^\dagger$  ( $\hat{b}_{v\mathbf{k}}$ ) are the creation (annihilation) operators for electrons and holes, respectively,  $\epsilon_{n\mathbf{k}}$  is the eigenvalue of  $H_0$ , and  $V_{\mathbf{q}}^{cc',vv'}$  is the screened Coulomb interaction in the basis of eigenstates of  $H_0$ . Here,  $v$  and  $c$  are band indices for valence band and conduction band,  $\mathbf{k}$  is the crystal momentum, and  $\mathbf{q}$  denotes the Fourier component for Coulomb interaction [12, 14]. Note that  $\hat{b}_{v\mathbf{k}}^\dagger \equiv \hat{c}_{v-\mathbf{k}}$ . Then, in order to calculate the total carrier generation rate  $\Gamma^{\alpha\beta}(\omega)$ , we need to evaluate the retarded momentum-momentum correlation function  $\chi^{\alpha\beta}(\omega)$  as prescribed in [8]:

$$\Gamma^{\alpha\beta}(\omega) = -\frac{2}{\hbar} \text{Im} [\chi^{\alpha\beta}(\omega)] \left(\frac{e}{m\omega}\right)^2 E_\alpha E_\beta. \quad (4)$$

$$\chi_T^{\alpha\beta}(i\omega_n) = -\frac{1}{\hbar} \sum_{\mathbf{k}cv} \langle v\mathbf{k} | \hat{p}^\alpha | c\mathbf{k} \rangle D_{cv,\mathbf{k}}^\beta(i\omega_n) \quad (5)$$

where

$$D_{cv,\mathbf{k}}^\beta(i\omega_n) = \sum_{\mathbf{k}'c'v'} \langle c'\mathbf{k}' | \hat{p}^\beta | v'\mathbf{k}' \rangle \times \int_0^{\hbar/k_B T} d\tau e^{i\omega_n \tau} \left\langle \hat{T}_\tau \hat{b}_{v-\mathbf{k}}(\tau) \hat{c}_{c\mathbf{k}}(\tau) \hat{c}_{c'\mathbf{k}'}^\dagger(0) \hat{b}_{v'-\mathbf{k}'}^\dagger(0) \right\rangle. \quad (6)$$

Here, momentum-momentum correlation functions  $\chi^{\alpha\beta}(\omega)$  (real-time, retarded) and  $\chi_T^{\alpha\beta}(i\omega_n)$  (imaginary-time) can be related via an analytical continuation:  $\chi^{\alpha\beta}(\omega) = \chi_T^{\alpha\beta}(i\omega_n \rightarrow \omega + i0^+)$  [14, 15], and from Eq. 5 we can see that  $\Gamma^{\alpha\beta}(\omega)$  can be decomposed as  $\Gamma^{\alpha\beta}(\omega) = \sum_{cv,\mathbf{k}} \Gamma_{cv,\mathbf{k}}^{\alpha\beta}(\omega)$ . The correlation function in Eq. 6 is evaluated under the full Hamiltonian

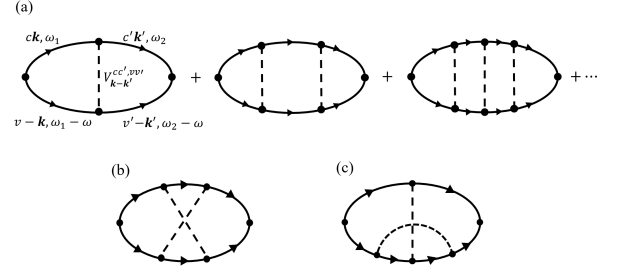


FIG. 1. Feynman diagrams for electron-hole interaction. For a semiconductor, only ladder diagrams in (a) will contribute to asymmetric scattering.

$H = H_0 + V_{\text{int}}$ , so to calculate it perturbatively, we carry out a diagrammatic approach by expressing each perturbation term as a Feynman diagram. Only ladder diagrams will contribute to the asymmetric scattering for insulators ([14, 16, 17]). However, due to the long-range character of the Coulomb interaction, we cannot simply retain the lowest-order term. Thus, we need to sum up all orders of ladder diagrams as shown in Fig. 1.

After applying the Feynman rule for each diagram and going through a fair amount of algebra [17], the sum of the ladder diagrams can be written as:

$$\mathbf{D}_{cv,\mathbf{k}}(\omega) = \sum_{n=0}^{\infty} \mathbf{D}_{cv,\mathbf{k}}^{(n)}(\omega) = i \frac{\tilde{\mathbf{P}}_{cv,\mathbf{k}}(\omega)}{\omega + \epsilon_{v\mathbf{k}}/\hbar - \epsilon_{c\mathbf{k}}/\hbar + i0^+}, \quad (7)$$

and

$$\tilde{\mathbf{P}}_{cv,\mathbf{k}}(\omega) = \langle c\mathbf{k} | \hat{\mathbf{p}} | v\mathbf{k} \rangle + \sum_{\mathbf{k}'c'v'} \frac{i}{\hbar} \frac{V_{\mathbf{k}-\mathbf{k}'}^{cc',vv'}}{\omega + \epsilon_{v'\mathbf{k}'}/\hbar - \epsilon_{c'\mathbf{k}'}/\hbar + i0^+} \tilde{\mathbf{P}}_{c'v',\mathbf{k}'}(\omega). \quad (8)$$

This summation was first carried out in [16], where the effective mass approximation was assumed and the  $\mathbf{k}$ -dependence of the momentum matrix was neglected. The more general Eq. 8 can be numerically solved for each frequency  $\omega$  on a  $\mathbf{k}$ -grid, so together with Eq. 5, Eq. 7, and Eq. 8, the carrier generation rate  $\Gamma_{cv,\mathbf{k}}^{\alpha\beta}(\omega)$  can be calculated from first principles. We note here that a similar derivation for  $\Gamma_{cv,\mathbf{k}}^{\alpha\beta}(\omega)$  has been carried out in [7, 9], and fairly good agreement with experiments has been achieved. However, their focus is exclusively on the near-band-edge states, and only first-order perturbation is used when treating  $\mathbf{k}$  points farther away from the band edge. Therefore, our derivation has the advantage of incorporating more states throughout the whole Brillouin zone and giving a current response for a broader frequency range.

*Many-body Approach.*— Here we present another approach to calculate the carrier generation rate, in which

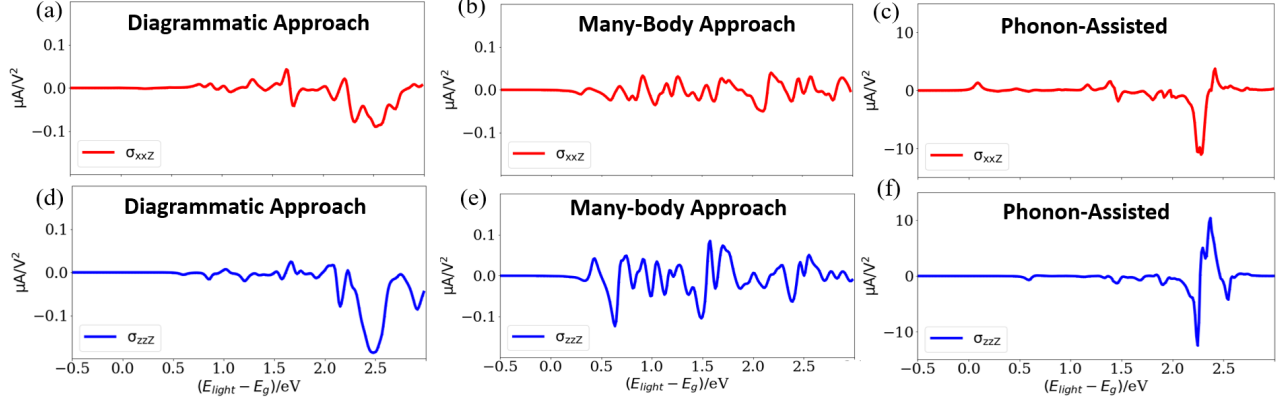


FIG. 2. First-principles results of ex-BC for tetragonal BaTiO<sub>3</sub>. Note the scale difference in these figures. (a)-(c) are the  $xxZ$  component of the current response tensors, and (d)-(f) are the  $zzZ$  component. Both the diagrammatic approach (a,d) and the many-body approach (b,e) give results of similar magnitude, two orders smaller than the phonon-assisted ballistic current as shown in (c) and (f) (reproduced from [8]).

the wave functions of exciton states  $|S\rangle$  are computed explicitly from many-body theory. According to Fermi's golden rule [18], the total carrier generation rate due to light absorption can be expressed as:

$$\Gamma^{\alpha\beta}(\omega) = \frac{2\pi}{\hbar} \left( \frac{e}{m\omega} \right)^2 E^\alpha E^\beta \times \sum_S \langle 0 | \hat{p}^\alpha | S \rangle \langle S | \hat{p}^\beta | 0 \rangle \delta(\Omega^S - \hbar\omega), \quad (9)$$

where  $\Omega^S$  is the excitation energy and  $|0\rangle$  is the ground state of the system. The exciton states can be expressed by the linear combination of electron-hole pair states [13]:

$$|S\rangle = \sum_{v\mathbf{c}\mathbf{k}} A_{v\mathbf{c}\mathbf{k}}^S |v\mathbf{c}\mathbf{k}\rangle = \sum_{v\mathbf{c}\mathbf{k}} A_{v\mathbf{c}\mathbf{k}}^S \hat{c}_{\mathbf{c}\mathbf{k}}^\dagger \hat{b}_{v-\mathbf{k}}^\dagger |0\rangle, \quad (10)$$

and we call  $A_{v\mathbf{c}\mathbf{k}}$  the exciton wave functions. By substituting Eq. (10) into Eq. (9), we can rewrite the carrier generation rate as:

$$\Gamma^{\alpha\beta}(\omega) = \frac{2\pi}{\hbar} \left( \frac{e}{m\omega} \right)^2 E^\alpha E^\beta \times \sum_{v\mathbf{c}\mathbf{k}} \sum_S |A_{v\mathbf{c}\mathbf{k}}^S|^2 \langle v\mathbf{k} | \hat{p}^\alpha | \mathbf{c}\mathbf{k} \rangle \langle \mathbf{c}\mathbf{k} | \hat{p}^\beta | v\mathbf{k} \rangle \delta(\Omega^S - \hbar\omega), \quad (11)$$

from which we can see again that the overall generation rate can be split into  $\sum_{cv,\mathbf{k}} \Gamma_{cv,\mathbf{k}}^{\alpha\beta}(\omega)$ . Eq. (11) is to be contrasted with the carrier generation rate (transition rate) in a more well-known form that does not take electron-hole interaction into account:

$$\Gamma_{cv,\mathbf{k}}^{\alpha\beta,\text{no-eh}}(\omega) = \frac{2\pi}{\hbar} \left( \frac{e}{m\omega} \right)^2 E^\alpha E^\beta \times \sum_{v\mathbf{c}\mathbf{k}} \langle v\mathbf{k} | \hat{p}^\alpha | \mathbf{c}\mathbf{k} \rangle \langle \mathbf{c}\mathbf{k} | \hat{p}^\beta | v\mathbf{k} \rangle \delta(E_{\mathbf{c}\mathbf{k}} - E_{v\mathbf{k}} - \hbar\omega). \quad (12)$$

Clearly,  $\Gamma_{cv,\mathbf{k}}^{\alpha\beta,\text{no-eh}}(\omega)$  together with  $\beta\alpha$  component is symmetric under  $\mathbf{k} \Leftrightarrow -\mathbf{k}$  and therefore gives no net current. Thus, it is the asymmetry lying in the exciton wave functions  $A_{v\mathbf{c}\mathbf{k}}^S$  that will make the carrier generation at  $\mathbf{k}$  and  $-\mathbf{k}$  unequal.

The exciton wave functions and excitation energies can be obtained by solving the *Bethe-Salpeter Equation* (BSE):

$$(E_{\mathbf{c}\mathbf{k}} - E_{v\mathbf{k}}) A_{v\mathbf{c}\mathbf{k}}^S + \sum_{v'\mathbf{c}'\mathbf{k}'} \langle v\mathbf{c}\mathbf{k} | K^{eh} | v'\mathbf{c}'\mathbf{k}' \rangle = \Omega^S A_{v\mathbf{c}\mathbf{k}}^S, \quad (13)$$

where the kernel  $K^{eh}$  describes the electron-hole interaction, whose explicit form and technical details have been discussed extensively in [19]. Once the BSE is solved, we can use  $A_{v\mathbf{c}\mathbf{k}}^S$  and  $\Omega^S$  to calculate the carrier generation rate  $\Gamma_{cv,\mathbf{k}}^{\alpha\beta}(\omega)$  via Eq. (11).

*First-Principles Results.*— The two approaches can be implemented numerically to calculate carrier generation rate  $\Gamma_{cv,\mathbf{k}}^{\alpha\beta}(\omega)$ , and together with Eq. (1), the exciton ballistic current for real materials can also be calculated via first principles. To demonstrate this capability and in order for better comparison, we choose the prototypical BPVE material tetragonal BaTiO<sub>3</sub> due to the availability of experimental BPVE data [20, 21] as well as first-principles results of shift current [5, 6] and ph-BC. [8] In addition to BaTiO<sub>3</sub>, we also applied the same calculation to the 2D material MoS<sub>2</sub>, which has a strong exciton effect [22] and is expected to possess a more obvious ex-BC. The structural data are obtained from [23, 24]. For monolayer MoS<sub>2</sub>, since the out-of-plane direction does not have a well-defined lattice parameter  $c$ , we have multiplied its response tensors by  $c$  to make it well-defined for 2D systems [25].

We perform density functional theory (DFT) calculations using the QUANTUM ESPRESSO package. [26,

27] The generalized-gradient approximation exchange-correlation functional and norm-conserving pseudopotentials produced by the OPIUM package are used. [28–30] The convergence threshold for self-consistent calculations was  $1 \times 10^{-8}$  Ry/cell. *GW* and BSE calculations were performed using BERKELEYGW [19, 31, 32] to find the exciton wave functions. For illustrative purposes, all quantities are sampled on an  $8 \times 8 \times 8$  k-grid for BaTiO<sub>3</sub> and  $16 \times 16 \times 1$  for MoS<sub>2</sub> [33], and denser grids can be used for finer spectral features. In the *GW* calculations, the cut-off of the dielectric matrix was set as 10 Ry. For BaTiO<sub>3</sub>, we include 20 valence and 200 conduction bands, whereas for MoS<sub>2</sub>, 13 valence and 130 conduction bands are included. To construct the  $K^{eh}$  in the BSE, 6 valence and 6 conduction bands are used in BaTiO<sub>3</sub> and 9 valence and 9 conduction bands are used in MoS<sub>2</sub>. The relaxation times for BaTiO<sub>3</sub> and MoS<sub>2</sub> are chosen to be 2 fs and 100 fs, respectively, either from first principle simulations by considering that the relaxation is from electron-phonon coupling [8] or from experiments [34]. For both materials, a 0.1 eV broadening parameter is adopted for the delta function.

The results for BaTiO<sub>3</sub> are shown in Fig. 2. It can be seen that both approaches will give ex-BC current of similar magnitude, though their spectral features differ somewhat and it is hard to pinpoint the corresponding peaks in two methods due to the high spectral density. The ex-BC magnitudes are 1–2 orders smaller than the shift current and ph-BC. From this, we can see that even though we have considered infinite order of e-h scattering perturbatively, their summation converges to a small value compared with ph-BC where only the lowest-order electron-phonon interaction is taken into account. Hence, for BaTiO<sub>3</sub>, the electron-hole interaction only has a minor contribution to the asymmetric scattering, and one has to resort to other scattering mechanisms, such as defect- or disorder-induced scattering in order to explain the discrepancy between experiments and simulations. In addition, combined with our previous work [5, 8], we showed that for BaTiO<sub>3</sub> the shift current is indeed the dominating mechanism of BPVE in the energy range right above the band edge.

To see if electron-hole interaction has a greater impact on the asymmetric scattering for 2D materials which are expected to have strong exciton effects, we compared the ex-BC of MoS<sub>2</sub> with its shift current, which has been reported to be large. In Fig. 3, it can be seen that even though the ex-BC indeed constitutes a larger proportion in overall BPVE than that of BaTiO<sub>3</sub> due to a larger momentum relaxation time [34], its magnitude is still smaller than the shift current. Noticeably, the smaller number of features in MoS<sub>2</sub> enables us to see clearly that the first few features in Fig. 3(a) and Fig. 3(b) follow the same trend, demonstrating both methods to be equally capable of giving at least qualitative predictions of ex-BC. Since the longer relaxation time, rather than a higher

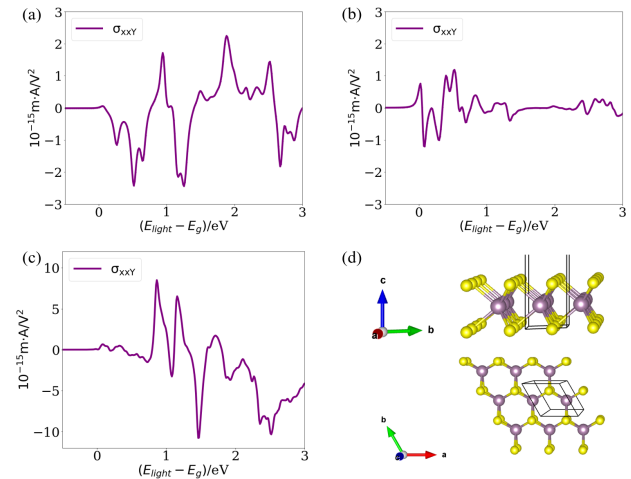


FIG. 3. First-principles results for MoS<sub>2</sub>. (a) Exciton ballistic current ex-BC from the diagrammatic approach. (b) ex-BC from the many-body approach. (c) Shift current as reproduced from [6]. (d) Atomic structure of MoS<sub>2</sub>. The MoS<sub>2</sub> has a larger ex-BC due to the longer relaxation time[34], but its asymmetric carrier generation rate is not necessarily large, even though strong exciton binding is expected for this material.

asymmetric carrier generation rate, causes the larger ex-BC in MoS<sub>2</sub>, this shows that cancellations between various orders of ladder diagrams will make its overall contribution less appreciable, and any proper treatment of the Coulomb interaction should contain more than the lowest-order perturbation term.

*Discussion and Conclusion.*— The first-principles results for BaTiO<sub>3</sub> and MoS<sub>2</sub> show clearly that ex-BC is a minor contribution to the overall BPVE in these materials, so unlike the ph-BC which can greatly enhance the agreement between the theoretical BPVE spectra and experimental ones, the ex-BC is less significant, and perhaps it can be safely neglected when analyzing the constituents of experimental photocurrent for materials without a strong exciton effect. As a result, we would expect that defect or disorder scattering could make a stronger contribution to BPVE, not only because it can induce asymmetric carrier generation, but also due to the coordinate shift that accompanies any scattering process, which resembles the shift current mechanism [35, 36].

We would also like to comment on the relations between the two approaches we presented. The diagrammatic approach starts from a single-particle picture and treats the electron-hole interaction in a phenomenological way, whereas the many-body approach is based on the full many-body picture (Green’s function formalism and Hedin’s equations) and can be reduced to a two-particle equation in the second iteration of solving Hedin’s equations. [10] A connection between the two approaches has been attempted by [37], and they showed that when taking the effective-mass approximation, the

two methods can be proved to be equivalent. When the full  $\mathbf{k}$ -dependence and multi-band nature are recovered, however, it becomes unclear how the two methods correspond to each other. Therefore, the different nature at the very beginning makes it difficult to pinpoint exactly what causes the differences in the results.

In general, we expect the many-body approach should give more accurate results for the following reasons: 1. The diagrammatic approach lacks the electron-hole renormalization of the band structure since the most accurate band energies possible are still from the GW approximation that adopts quasi-single-particle picture, and they are not necessarily the same as the BSE eigenvalues. 2. The screening is more accurate in the many-body approach. In the diagrammatic approach, the screening is from the macroscopic dielectric constant  $\epsilon_0 = \epsilon_M(\omega = 0)$  that is  $\mathbf{G}$ -vector independent [38], whereas in the many-body approach the screening is from the static dielectric function  $\epsilon_{\mathbf{G}\mathbf{G}'}(\mathbf{q}, \omega = 0)$ , and this can be further improved by using the frequency-dependent dielectric function  $\epsilon_{\mathbf{G}\mathbf{G}'}(\mathbf{q}, \omega)$  [10]. 3. When arriving at the model Hamiltonian Eq. 2 and Eq. 3 that describes the diagrammatic approach, the use of DFT eigenstates as basis could include some information of two-particle interaction already (the exchange-correlation energy in Kohn-Sham equations), so adding a two-particle interaction to a formally non-interacting Hamiltonian expressed in this basis could result in extra error [12]. On the other hand, the many-body approach is formulated from the many-body Green's function formalism where the two-particle interaction is treated more systematically, so its physical picture should be more rigorous than that of diagrammatic approach [10].

Despite these, the similar magnitudes from these two methods demonstrate that the diagrammatic approach can at least give qualitative predictions of ex-BC, and in practice the implementation of the diagrammatic method is more computationally efficient than that of the many-body approach. So, the diagrammatic approach can work as a preliminary calculation to check the importance of exciton ballistic current in materials of interest. If the magnitude of current from this approach is large, then more accurate calculations from the many-body approach can be undertaken to get more predictive results.

To summarize, we employed two approaches to investigate the ballistic current from electron-hole scattering in a first principle way, which will be indispensable for a complete and quantitative understanding of various mechanisms to BPVE, and it could be a corner stone to resolve the long-standing debate over the relative importance of shift current and ballistic current in real materials. Following these two methods, we performed *ab initio* calculations on BaTiO<sub>3</sub> and MoS<sub>2</sub> to demonstrate the influence of ex-BC on BPVE. Our numerical results show that electron-hole scattering has a relatively small contribution to BPVE for these two materials compared

with shift current and phonon-assisted ballistic current, so more scattering mechanisms should be considered in order to better explain their experimental photocurrents. On the other hand, the two approaches presented here enable the numerical evaluation of the importance of eh-BC for any semiconductor, and they open up the possibility for *ab initio* prediction and design of materials with larger ex-BC.

*Acknowledgments.* This work was supported by the U.S. Department of Energy, Office of Science, Basic Energy Sciences, under Award # DE-FG02-07ER46431. Computational support was provided by the National Energy Research Scientific Computing Center (NERSC), a U.S. Department of Energy, Office of Science User Facility located at Lawrence Berkeley National Laboratory, operated under Contract No. DE-AC02-05CH11231. We acknowledge valuable discussions with Lingyuan Gao.

- 
- [1] V. I. Belinicher and B. I. Sturman, *Sov. Phys. USP.* **23**, 199 (1980).
  - [2] V. I. Belinicher, *Ferroelectrics* **83**, 29 (1988).
  - [3] J. E. Spanier, V. M. Fridkin, A. M. Rappe, A. R. Akbashev, A. Polemi, Y. Qi, Z. Gu, S. M. Young, C. J. Hawley, D. Imbrenda, G. Xiao, A. L. Bennett-Jackson, and C. L. Johnson, *Nature Photonics* **10**, 611 (2016).
  - [4] R. von Baltz and W. Kraut, *Phys. Rev. B* **23**, 5590 (1981).
  - [5] S. M. Young and A. M. Rappe, *Phys. Rev. Lett.* **109**, 116601 (2012).
  - [6] R. Fei, L. Z. Tan, and A. M. Rappe, *Physical Review B* **101**, 045104 (2020).
  - [7] B. I. Sturman and V. M. Fridkin, *The Photovoltaic and Photorefractive Effects in Noncentrosymmetric Materials*, edited by G. W. Taylor, *Ferroelectricity and Related Phenomena*, Vol. 8 (Gordon and Breach Science Publishers, 1992).
  - [8] Z. Dai, A. M. Schankler, L. Gao, L. Z. Tan, and A. M. Rappe, *Physical Review Letters* **126**, 177403 (2021).
  - [9] V. I. Shelest and M. V. Entin, *Soviet Physics Semiconductors-USSR* **13**, 1353 (1979).
  - [10] G. Onida, L. Reining, and A. Rubio, *Rev. Mod. Phys.* **74**, 601 (2002).
  - [11] R. S. Knox, *Solid State Phys.* **5** (1963).
  - [12] M. Combescot and S.-Y. Shiao, *Excitons and Cooper pairs: two composite bosons in many-body physics* (Oxford University Press, 2015).
  - [13] M. Rohlfing and S. G. Louie, *Physical review letters* **81**, 2312 (1998).
  - [14] G. D. Mahan, *Many-particle physics* (Springer Science & Business Media, 2013).
  - [15] R. A. Jishi, *Feynman diagram techniques in condensed matter physics* (Cambridge University Press, 2013).
  - [16] G. D. Mahan, *Physical Review* **153**, 882 (1967).
  - [17] See Supplemental Material at [URL will be inserted by publisher] for the derivation leading to the summation of the ladder diagrams, the discussion about non-ladder diagrams, and the band structures for BaTiO<sub>3</sub> and MoS<sub>2</sub>, which includes Refs. [12, 15, 38].

- [18] F. Bassani, G. P. Parravicini, R. A. Ballinger, and J. L. Birman, *Physics Today* **29**, 58 (1976).
- [19] J. Deslippe, G. Samsonidze, D. A. Strubbe, M. Jain, M. L. Cohen, and S. G. Louie, *Computer Physics Communications* **183**, 1269 (2012).
- [20] W. T. H. Koch, R. Munser, W. Ruppel, and P. Wurfel, *Solid State Communications* **17**, 847 (1975).
- [21] W. T. H. Koch, R. Munser, W. Ruppel, and P. Wurfel, *Ferroelectrics* **13**, 305 (1976).
- [22] K. Wang and B. Paulus, *Physical Chemistry Chemical Physics* **22**, 11936 (2020).
- [23] R. H. Buttner and E. N. Maslen, *Acta Crystallographica Section B: Structural Science* **48**, 764 (1992).
- [24] A. M. Schankler, L. Gao, and A. M. Rappe, *The Journal of Physical Chemistry Letters*, 1244 (2021).
- [25] H. Wang and X. Qian, *Nano Lett.* **17**, 5027 (2017).
- [26] P. Giannozzi, S. Baroni, N. Bonini, M. Calandra, R. Car, C. Cavazzoni, D. Ceresoli, G. L. Chiarotti, M. Cococcioni, I. Dabo, A. D. Corso, S. de Gironcoli, S. Fabris, G. Fratesi, R. Gebauer, U. Gerstmann, C. Gougoussis, A. Kokalj, M. Lazzeri, L. Martin-Samos, N. Marzari, F. Mauri, R. Mazzarello, S. Paolini, A. Pasquarello, L. Paulatto, C. Sbraccia, S. Scandolo, G. Sclauzero, A. P. Seitsonen, A. Smogunov, P. Umari, and R. M. Wentzcovitch, *J. Phys.: Condens. Matter* **21**, 395502 (1 (2009)).
- [27] P. Giannozzi, O. Andreussi, T. Brumme, O. Bunau, M. B. Nardelli, M. Calandra, R. Car, C. Cavazzoni, D. Ceresoli, M. Cococcioni, N. Colonna, I. Carnimeo, A. D. Corso, S. de Gironcoli, P. Delugas, R. A. DiStasio, A. Ferretti, A. Floris, G. Fratesi, G. Fugallo, R. Gebauer, U. Gerstmann, F. Giustino, T. Gorni, J. Jia, M. Kawamura, H.-Y. Ko, A. Kokalj, E. Küçükbenli, M. Lazzeri, M. Marsili, N. Marzari, F. Mauri, N. L. Nguyen, H.-V. Nguyen, A. O. de-la Roza, L. Paulatto, S. Poncé, D. Rocca, R. Sabatini, B. Santra, M. Schlipf, A. P. Seitsonen, A. Smogunov, I. Timrov, T. Thonhauser, P. Umari, N. Vast, X. Wu, and S. Baroni, *Journal of Physics: Condensed Matter* **29**, 465901 (2017).
- [28] J. P. Perdew, K. Burke, and M. Ernzerhof, *Phys. Rev. Lett.* **77**, 3865 (1 (1996)).
- [29] A. M. Rappe, K. M. Rabe, E. Kaxiras, and J. D. Joannopoulos, *Phys. Rev. B Rapid Comm.* **41**, 1227 (1990).
- [30] N. J. Ramer and A. M. Rappe, *Phys. Rev. B* **59**, 12471 (1999).
- [31] M. S. Hybertsen and S. G. Louie, *Phys. Rev. B* **34**, 5390 (1986).
- [32] M. Rohlfing and S. G. Louie, *Phys. Rev. B.* **62**, 4927 (2000).
- [33] H. J. Monkhorst and J. D. Pack, *Phys. Rev. B* **13**, 5188 (1976).
- [34] R. Fei, W. Song, and L. Yang, *Physical Review B* **102**, 035440 (2020).
- [35] N. A. Sinitsyn, Q. Niu, and A. H. MacDonald, *Physical Review B* **73**, 075318 (2006).
- [36] C. Xiao, Z. Z. Du, and Q. Niu, *Physical Review B* **100**, 165422 (2019).
- [37] L. J. Sham and T. M. Rice, *Physical Review* **144**, 708 (1966).
- [38] A. Laturia, M. L. V. de Put, and W. G. Vandenberghe, *npj 2D Materials and Applications* **2**, 6 (1 (2018)).